

In-situ application of colloidal activated carbon for PFAS-contaminated soil and groundwater: A Swedish case study

Georgios Niarchos¹  | Lutz Ahrens² | Dan Berggren Kleja³ | Gareth Leonard⁴ | Jim Forde⁴ | Jonny Bergman⁵ | Erik Ribeli⁶ | Matilda Schütz⁶ | Fritjof Fagerlund¹

¹Department of Earth Sciences, Uppsala University, Uppsala, Sweden

²Department of Aquatic Sciences and Assessment, Swedish University of Agricultural Sciences (SLU), Uppsala, Sweden

³Department of Soil and Environment, Swedish University of Agricultural Sciences (SLU), Uppsala, Sweden

⁴REGENESIS Bioremediation Products Ltd, Ireland

⁵RGS Nordic, Göteborg, Sweden

⁶NIRAS, Stockholm, Sweden

Correspondence

Georgios Niarchos, Department of Aquatic Sciences and Assessment, Swedish University of Agricultural Sciences (SLU), P.O. Box 7050, SE-750 07, Uppsala, Sweden.
Email: georgios.niarchos@slu.se

Funding information

Swedish Geotechnical Institute

Abstract

Soil and groundwater contamination by per- and polyfluoroalkyl substances (PFAS) has been a significant concern to human health and environmental quality. Remediation of contaminated sites is crucial to prevent plume expansion but can prove challenging due to the persistent nature of PFAS combined with their high aqueous mobility. In this case study, we investigated the potential of colloidal activated carbon (CAC) for soil stabilization at the pilot scale, aiming to entrap PFAS and prevent their leaching from soil into groundwater. Monitoring of the site revealed the presence of two potential sources of PFAS contamination at concentrations up to $23 \mu\text{g L}^{-1}$ for Σ_{11} PFAS in groundwater. After CAC application, initial results indicated a 76% reduction of Σ_{11} PFAS and high removal rates for long-chain PFAS, such as perfluorooctane sulfonic acid and perfluorooctanoic acid. A spike in concentrations was noticed 6 months after injection of CAC, showing a rebound of the plume and a reduction of treatment effectiveness. Based on long-term monitoring data, the treatment effectiveness for Σ_{11} PFAS dropped to 52%. The rebound of concentrations was attributed to the plume bypass of the barrier due to the presence of high conductivity zones, which likely occurred because of seasonal changes in groundwater flow directions or the CAC application at the site. This demonstrates the need for a detailed and accurate hydrogeological understanding of contaminated sites before designing and applying stabilization techniques, especially at sites with high geologic and hydrologic complexity. The results herein can serve as a guideline for treating similar sites and help avoid potential pitfalls of remedial efforts.

1 | INTRODUCTION

Per- and polyfluoroalkyl substances (PFAS) encompass a large group of emerging anthropogenic organic contaminants. Increased public concern and new data on health effects associated with PFAS (ATDSR, 2018) have caused a resurgence of regulatory attention and scientific response

in recent years (Brennan et al., 2021). While stringent regulations aim to reduce the widespread occurrence of PFAS, their usage is still high, with a production shift to short-chain PFAS and new PFAS being introduced into the global market (OECD, 2018). Wang et al. (2014) have projected the global emissions to water and air of C_4 – C_{14} perfluorocarboxylic acids (PFCA) to be between 20 and 6420 tonnes during 2016–2030, which,

This is an open access article under the terms of the Creative Commons Attribution License, which permits use, distribution and reproduction in any medium, provided the original work is properly cited.

© 2023 The Authors. *Remediation* published by Wiley Periodicals LLC.

when compared with previous decades, is a reduced, yet significant, quantity. Meanwhile, the extent of environmental PFAS contamination is being documented worldwide. As of December 2021, 1782 PFAS-contaminated sites were registered in the United States, 78% of which included groundwater contamination (EWG & SSEHRI, 2019). In Sweden, a nationwide study in 2016 identified more than 2000 potential sources of PFAS contamination, leading to high PFAS levels ($>90 \text{ ng L}^{-1}$) in drinking water (Swedish Environmental Protection Agency, 2016). Most of these sources were areas close to firefighting training stations, as is often the case due to the historical PFAS use in aqueous film-forming foams (AFFF) (Dauchy et al., 2017). The Swedish guidelines for PFAS in groundwater mandate a safe limit of 45 ng L^{-1} for perfluorooctane sulfonic acid (PFOS) and a total of 90 ng L^{-1} for the sum of 11 PFAS ($\sum_{11} \text{PFAS}$), namely perfluorobutanoic acid (PFBA), perfluoropentanoic acid (PFPeA), perfluorohexanoic acid (PFHxA), perfluoroheptanoic acid (PFHpA), perfluorooctanoic acid (PFOA), perfluorononanoic acid (PFNA), perfluorodecanoic acid (PFDA), perfluorobutane sulfonic acid (PFBS), perfluorohexanesulfonic acid (PFHxS), PFOS, and 6:2 fluorotelomer sulfonate (FTSA) (Pettersson et al., 2015). Globally, reported PFAS concentrations in contaminated soils are typically at the ppm level, with higher concentrations closer to the soil surface (Brusseau et al., 2020). In Swedish background soils, Söregård et al. (2022) recently estimated that a total load of 17 tons exists for 16 out of 28 screened PFAS, namely PFHpA, PFOA, PFNA, PFDA, perfluoroundecanoic acid (PFUnDA), perfluorododecanoic acid (PFDoDA), perfluorotridecanoic acid (PFTriDA), perfluorotetradecanoic acid (PFTeDA), perfluorohexadecanoic acid (PFHxDA), perfluorooctadecanoic acid (PFOcDA), PFBS, PFHxS, PFOS, 6:2 FTSA, perfluorooctanesulfonamide (FOSA), and perfluorooctane sulfonamidoacetic acid (FOSAA). Therefore, soils can act as both significant sources and sinks of PFAS contamination, accentuating the need for effective soil treatment methods.

In recent years, various remediation strategies for PFAS-impacted soils have been studied, including destruction (e.g., thermal destruction [Crownover et al., 2019; Söregård et al., 2020]), removal (e.g., electrokinetic removal [Niarchos et al., 2022; Söregård et al., 2019]), phytoremediation (Huang et al., 2021), and stabilization techniques. Many of the available technologies, such as destruction methods, are typically applied ex-situ resulting in higher costs, and often result in by-product creation (Ross et al., 2018). In-situ stabilization is currently the most mature technology for remediation of PFAS-contaminated soils and has proven to be cost-efficient and effective for PFAS removal (Darlington et al., 2018; Høisæter et al., 2021; Mahinroosta & Senevirathna, 2020; Ross et al., 2018). Stabilization involves the addition of fixation agents in the subsurface to entrap contaminants and prevent their leaching from contaminated soils to groundwater. Different materials can be used as fixation agents, but commonly these are activated carbons in various forms, such as granular activated carbon (GAC) or powdered activated carbon (PAC). One novel material is colloidal activated carbon (CAC), which comprises activated carbon particles of diameter $1\text{--}2 \mu\text{m}$ suspended in a solution with polymers, that can therefore be injected into the subsurface (Mackenzie et al., 2008). Laboratory-scale studies have demonstrated good efficiency of CAC for PFAS treatment, with solid-liquid partitioning coefficients (K_d) ranging between 10^2 and 10^5 ,

with long-chain PFAS having the highest K_d values (Niarchos et al., 2022; Sorengard et al., 2019). However, most of these studies have been carried out at the bench-scale and under well-controlled conditions, while field-scale systematic applications are still in a nascent stage. Recently, McGregor (2020) studied the application of CAC in a sand aquifer and showed a significant reduction of PFAS concentrations in groundwater to below 30 ng L^{-1} , which lasted over 1.5 years, exhibiting better performance than PAC, ion-exchange resins, and biochar. However, another study showed that heterogeneity can have an impact on the CAC distribution, with low conductivity zones and bedrock fractures exhibiting difficulties and lower treatment capacities than sandy aquifers (McGregor & Benevenuto, 2021). Therefore, the effectiveness of stabilization with CAC can be site-specific.

The treatment effectiveness also depends on the intrinsic properties of PFAS and their structure, principally their chain length and functional group. The sorption behavior of PFAS is primarily governed by hydrophobic and electrostatic interactions (Du et al., 2014). The length of the perfluoroalkyl tail is directly correlated with adsorption strength, since longer-chain PFAS have a higher hydrophobicity (Guelfo & Higgins, 2013; Higgins & Luthy, 2006). Consequently, short-chain PFCA and perfluorosulfonates (PFSA) are expected to be more mobile in the subsurface and less responsive to stabilization with activated carbons. Furthermore, PFSA can reportedly sorb more strongly than PFCA of equivalent chain length (Higgins & Luthy, 2006; Li et al., 2019) as a result of their different functional head groups.

Remediation of contaminated soils can be challenging due to PFAS bonding with soil particles and humus, combined with their high aqueous mobility and stability against degradation, rendering their elimination difficult. Another obstacle is the significant number of different PFAS, including PFAS precursors, complicating the characterization and remediation of contaminated sites. Lastly, the presence of co-contaminants, such as nonaqueous phase liquids, which are common at PFAS-impacted locations, can affect the transport behavior of PFAS (Guelfo & Higgins, 2013).

In this study, a pilot-scale field experiment was carried out at a PFAS-impacted site located in central Sweden to investigate the potential of stabilization as a remediation technique and ascertain its effectiveness. A barrier of CAC was constructed using direct-push technology to prevent the spread of PFAS in the groundwater and further to nearby surface water bodies. The main objectives of this study were to ascertain the effectiveness of CAC stabilization on PFAS leaching and investigate the technology's shortcomings and uncertainties, specifically in the case of a hydrogeologically complex site.

2 | MATERIALS AND METHODS

2.1 | Investigation site

The investigation site was located 3.5 km southeast of the town of Arboga in central Sweden ($59^{\circ}23'14.3973'' \text{ N}$, $15^{\circ}53'50.6352'' \text{ E}$). The nearest protection area is a nature reserve, located approximately 3 km northeast of the site. Historically, firefighting training

was conducted at the site in a zone of circa 600 m² (Figure 1). Training activities occurred from the 1950s until the 1990s and they involved pouring aviation fuel on pits that were dug into the ground or on metal plates, igniting it, and then extinguishing it with PFAS-containing AFFF. The exact type and amount of the extinguishing agents that were used are unknown. The building south of the firefighting training zone was also used for indoor training (smoke divers), while the other buildings served as storage facilities and as such, are potential contributors to the site's contamination.

Early monitoring of the investigation site in 2015 revealed the presence of PFAS in soil, groundwater, and surface water (Supporting Information: Tables S1 and S2). PFAS were detected in a shallow stream flowing through the area, with PFOS concentrations exceeding the Annual Average Environmental Quality Standard (AA-EQS) of the EU Water Framework Directive (0.65 ng L⁻¹) (The European Parliament and the Council of the European Union, 2020), indicating the leaching of the contaminants from the soil through infiltrating rainwater or groundwater flow. There was also an open ditch situated in the proximity of well B2, which drains to the adjacent stream during wet periods. Several groundwater observation wells were installed to monitor the contaminant concentrations and groundwater levels, as can be seen in Figure 1. Based on the early monitoring and the historical uses of the site, the source zones of PFAS contamination were estimated (Supporting Information: Figure S1). However, the presence of additional source zones cannot be fully excluded.

The investigation area is situated primarily on top of postglacial fine clay, which is dense soil characterized by low permeability (Supporting Information: Figure S2). The aquifer is shallow and unconfined, lying on top of bedrock. Within a depth of 3 m from the surface the soil is silty clay, followed by a till layer closer to the bedrock, a frequent feature for Swedish soils (Hättestrand, 1997) (Supporting Information: Figure S3). The depth to the bedrock was mapped using soil-rock probing, showing depression of its surface along the stream (Supporting Information: Figure S4). The highest

bedrock point was at 15.5 m depth, compared with 11 m at the creek, indicating an average slope of ~20% in the bedrock surface from each side down to the creek in the east–west direction.

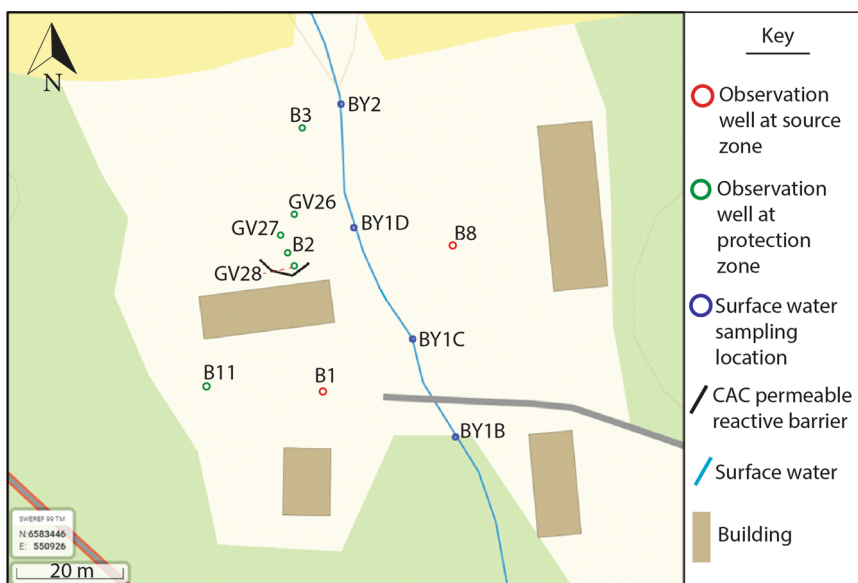
2.2 | Groundwater monitoring

Groundwater levels were monitored in all wells manually with sounding measurements at every sampling occasion (~every few months). Additionally, groundwater level loggers (Solinst LT F100/M30) were deployed in wells B1 and B3 for long-term monitoring of groundwater levels upstream and downstream of the protection zone. The groundwater levels measured by loggers were corrected for atmospheric pressure fluctuations by also logging barometric information above the groundwater surface (Solinst Barologger 5). Slug tests were used to estimate the hydraulic conductivity of the aquifer at the bottom of five observation wells by manually adding water and measuring the response time of the groundwater elevations (Supporting Information: Table S3).

The flow direction and velocity of the groundwater were estimated using iFLUX passive samplers from September to October 2019 (Supporting Information: Table S4). A total of eight sampling cartridges (five iFLUX Waterflux cartridges and three iFLUX Flow direction cartridges) were installed in three monitoring wells (B2, B24, and GV25) with a diameter of 41/50 cm (inner/outer) at depths between 2.40 and 3.40 m from the ground surface to measure water flux. Three of these cartridges were also used for directional measurements at a depth between 2.95 and 3.40 m. After 18 days of exposure, the cartridges were removed and estimations of flux and flow directions were recorded (Supporting Information: Table S4).

Groundwater samples were collected on several occasions during ~4 years and were sent to a commercial lab for PFAS content and chemical composition analysis. The wells were screened for PFAS below the water table, typically in the lowermost 1 m of the well

FIGURE 1 Overview of the contaminated site, including the main observation wells, stream sampling locations, and the CAC injection locations to create a permeable reactive barrier around well B2. The approximate identified PFAS source locations were around wells B1 and B8. A more detailed map of all the installed wells can be seen in Supporting Information: Figure S5. CAC, colloidal activated carbon; PFAS, per- and polyfluoroalkyl substances.



screens. The water in the wells was removed and replaced by fresh water from the surrounding formation before sampling, to ensure representative groundwater samples. In total, the following 11 PFAS were analyzed using a German standard method (DIN38407-42): 6:2 FTSA, PFBA, PFPeA, PFHxA, PFHpA, PFOA, PFNA, PFDA, PFBS, PFHxS, and PFOS. Method detection limits were between 0.3 and 20 ng L⁻¹. Chemical composition analysis involved pH, chemical oxygen demand, dissolved organic carbon, and metal and salt concentrations (for details, see Supporting Information: Table S5).

2.3 | Remediation strategy

The stabilization reagents used in this study were provided by Regenesis (PlumeStop®). A pilot-scale test was designed to control the PFAS plume using a permeable reactive barrier (PRB) upstream of well B2. The reason B2 was selected as the protection well was its location downstream of the main fire drill area (B1). Due to the possibility that the groundwater at B2 was also influenced by the contamination at the east side of the stream (B8), the PRB was designed in a U-shape to shield it from the sides and account for uncertainties in flow directions (Figure 2). Direct push injection of CAC in the subsurface was conducted using low pressure (1–1.5 bar) to minimize disturbances of the aquifer and opening of new flow channels by mixing the solution gradually with ambient groundwater. Both the clay and the underlying till unit were targeted for treatment by injecting CAC at depths between 2 and 4.8 m below the ground surface. More specifically, 2000 kg of CAC mixed with 1000 L of water were injected in total. The first two points had 1600 L of the mixture per point (10,000 ppm dose) and the remaining six points had 300 L of mixture per point (27,000 ppm dose). The exact volume of CAC at every depth interval is provided in Supporting Information: Table S6.

Calcium chloride (CaCl₂) was also injected in the proximity of the PRB and downgradient to restrict excessive PlumeStop® mobility. This decision was taken in response to observations of a very wide radius of

influence (>8 m) following initial PlumeStop® application at the first two injection points. The CaCl₂ was injected before CAC injection in low volumes (430 L per well) and 0.75 m downgradient of each subsequent CAC injection well to allow some distribution of CAC in the area before forming aggregates when in contact with CaCl₂. In total, 250 kg CaCl₂ mixed with 3000 L of water were used, (≈36 kg in 430 L per well). The injection occurred for 6 days between November 19, 2019 and November 28, 2019, and it was applied at 10 points with an approximate distance of 1.8 m between them. To monitor the concentration changes upstream and downstream, three additional observation wells were installed near B2 (GV26–28). To assess the CAC radius of influence, groundwater samples were collected from surrounding monitoring wells and window sampling was conducted around injection points, during and immediately after the injection, within and directly downstream of the barrier. The results showed mainly a spread of CAC in both till and clay layers, between injection points and directly downstream of the barrier at concentrations ranging from 700 to 3100 ppm (Supporting Information: Figure S6). During injection of CAC at the easternmost well, washing out of the material was noticed from the aquifer to the nearby stream and another injection point was applied in its proximity. However, the injected CAC went partly into the nearby stream and only a limited application of CAC could be performed in the easternmost points (Figure 2). This likely occurred due to connection with higher conductivity channels close to the bedrock or within bedrock fractures, leading to a barrier shorter than intended towards the east. Groundwater monitoring was conducted for approximately 2 years posttreatment (see Section 2.2) to assess the treatment's effectiveness.

3 | RESULTS AND DISCUSSION

3.1 | Groundwater levels and flow directions

Manual and logged groundwater levels compensated for barometric pressure are presented in Figure 3. The manual measurements

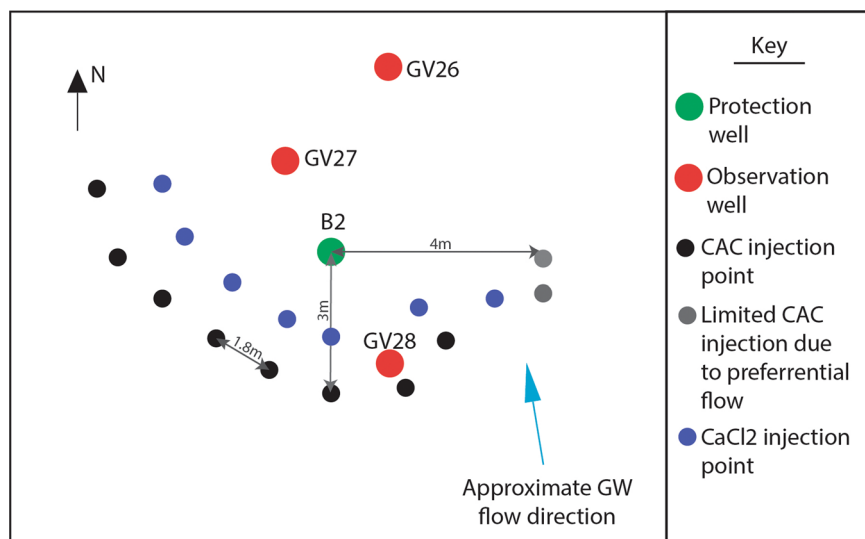


FIGURE 2 The permeable reactive barrier design. The arrangement includes injection wells for CAC and CaCl₂, as well as observation wells GV26, GV27, and GV28. CAC, colloidal activated carbon; CaCl₂, calcium chloride.

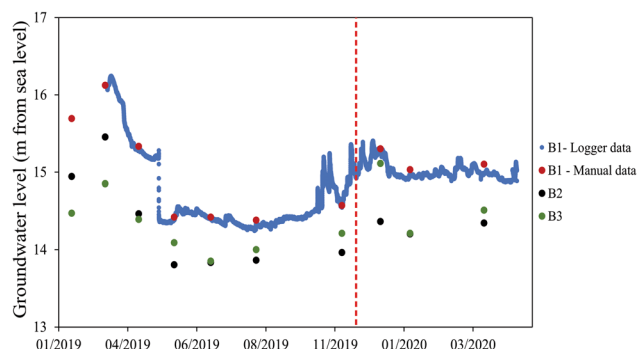


FIGURE 3 Groundwater level observations measured from sea level for upstream of protection well (well B1), protection well (well B2), and downstream of protection well (well B3). The red dashed line indicates the time of colloidal activated carbon injection.

showed a good match with the level logger data, validating their accuracy. Groundwater levels ranged between 14 and 16 m at the upstream well B1, 12.5–15.5 m at the protection well B2, and 13.8–15.8 m at the downstream well B3, showing a slight depression of the aquifer at well B2 along the south–north trajectory. The groundwater levels indicated a relatively flat water table from the south (B1) to north (B3) trajectory, with high seasonal variations at wells B1 and B3 (Figure 3). A snapshot of the groundwater levels during September 2020, revealed higher levels at the southernmost and easternmost of the investigation area (Supporting Information: Figure S7). Comparing groundwater levels to precipitation data (Supporting Information: Figure S8), it was evident that the groundwater levels were higher and fluctuated more during wet months (December–January) than in dry periods and during snow cover (February–April).

Based on the results of the iFLUX measurements, groundwater flow was directed toward the north–northwest at well B2 and northeast at adjacent wells (Supporting Information: Table S4). The water flux was estimated at $1.9 \text{ cm}^3 \text{ cm}^{-2} \text{ day}^{-1}$. It is important to note that these measurements were only for a limited timeframe (18 days), thus not capturing potential seasonal variations. The hydraulic conductivities (K) calculated from slug tests ranged from 10^{-7} to 10^{-9} m s^{-1} (Supporting Information: Table S3), which are typical values for tills or clay-rich soils (Duffield, 2019). Specifically, K was an order of magnitude higher on the north side of the area than in the south. There was also the possibility of a flow zone in bedrock fractures or at the soil–bedrock interface due to the higher conductivity of the till formation found in the deeper zones of the aquifer (Supporting Information: Figure S3).

3.2 | PFAS source characterization

Early PFAS analysis of groundwater samples revealed the occurrence of two primary source zones. The first was situated at well B1, located at the center of the firefighting training zone, while the other

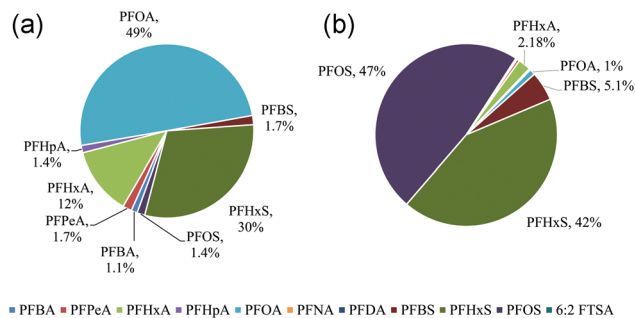


FIGURE 4 PFAS fingerprint at (a) the southern source (well B1) and (b) the eastern source (well B8). PFAS, per- and polyfluoroalkyl substances; PFBA, perfluorobutanoic acid; PFBS, perfluorobutane sulfonic acid; PFHpA, perfluoroheptanoic acid; PFHxA, perfluorohexanoic acid; PFHxS, perfluorohexanesulfonic acid; PFOA, perfluorooctanoic acid; PFOS, perfluorooctane sulfonic acid; PFPeA, perfluoropentanoic acid.

was on the east side of the stream, at well B8 (Figure 1). The two sources had different PFAS compositions (Figure 4), and the eastern source (B8) had PFAS levels almost twice as high. Specifically, well B1 contained mainly PFOA (50%), PFHxS (31%), and PFHxA (12%) and had an average $\sum_{11} \text{PFAS}$ concentration of $7810 \pm 3671 \text{ ng L}^{-1}$, while well B8 contained mainly PFOS (43%) and PFHxS (44%) with an average $\sum_{11} \text{PFAS}$ concentration of $19,900 \pm 195 \text{ ng L}^{-1}$. At both source zones, PFOS and $\sum_{11} \text{PFAS}$ levels were well beyond the safe limits for groundwater, 45 and 90 ng L^{-1} , respectively, according to Swedish guidelines (Pettersson et al., 2015). Long-chain PFAS, such as PFDA and PFNA, as well as 6:2 FTSA, were below method detection limits (0.30 ng L^{-1}). Around well B1, it was known that firefighting activities had taken place in the past, justifying the high PFAS levels; however, at well B8, the source of the contamination was uncertain but likely related to storage of PFAS-containing foams. The highest concentrations in the stream (58 ng L^{-1} for $\sum_{11} \text{PFAS}$) were measured at the location BY1D (Figure 1), which was situated between well B2 and the eastern source. At the protection well B2, 9 out of 11 PFAS were identified during early monitoring, with a concentration of $\sum_{11} \text{PFAS}$ of 860 ng L^{-1} .

PFAS fingerprints at the source zones (B1, B8) were stable over time (Supporting Information: Table S7). However, fluctuations of the groundwater concentrations were noticed at different sampling events. During wet periods, or periods of groundwater recharge (e.g., due to snowmelt), higher groundwater levels and an eventual dilution of PFAS occurred, resulting in lower groundwater concentrations; conversely, PFAS concentrations can appear higher during dry periods. It is therefore important to note that concentration changes due to groundwater level variability can cause some bias in the interpretation of treatment performance. Seasonal variations were noticeable, especially at the southern source (B1), while the highest concentrations were recorded just before CAC injection in early November 2019 (Figure 5). At the eastern source (B8), the variations were less pronounced; however, maximum concentrations

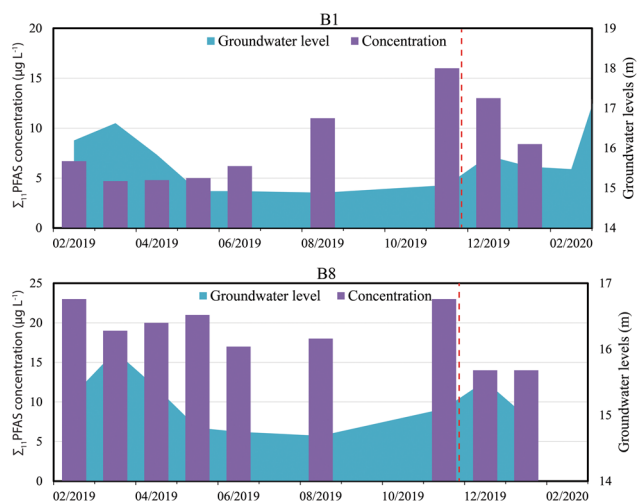


FIGURE 5 Seasonal variations of groundwater levels, measured from the mean sea level, versus concentrations for Σ_{11} PFAS at the source zones B1 (top) and B8 (bottom). The red dashed line indicates the time of CAC treatment application. CAC, colloidal activated carbon; PFAS, per- and polyfluoroalkyl substances.

were also recorded in November 2019. According to precipitation data, November is typically a relatively wet month (Supporting Information: Figure S8), therefore, the high concentrations could be explained by an increased infiltration rate that led to the transport of PFAS from shallow soil, deeper into the aquifer.

3.3 | Treatment effectiveness in the protection zone

At the protection well B2 and the downstream well B3, high concentrations of PFOS, PFHxS, and PFOA were detected before CAC injection, indicating a mixture of both the southern and eastern sources' PFAS fingerprints (Supporting Information: Figure S9). Similar concentrations were found at the nearby wells GV26, GV27, and GV28 located downgradient (Supporting Information: Figures S10 and S11). Specifically, at B2 PFOS comprised 40% of the total PFAS concentrations, while PFOA was merely 13%, suggesting a significant contribution of the easternmost source to PFAS contamination in the protection zone (Figure 4). It is important to note that the concentrations at the eastern source (B8) were higher, which would lead to a higher contribution compared to B1 due to dilution. A simple calculation of mixing the same amount of groundwater from the two sources results in the signature observed at B2 before CAC injection, meaning that the south and east sources contribute about equally to the concentrations that reach B2 (Supporting Information: Figure S12). The figures depicting PFAS data at the downstream well B3 showed a similar trend, with PFOS and PFHxS being the dominant constituents, at 43% and 35%, respectively (Supporting Information: Figure S9). High concentrations of PFOS and PFHxS were also found in the stream, indicating leaching from the eastern source (B8)

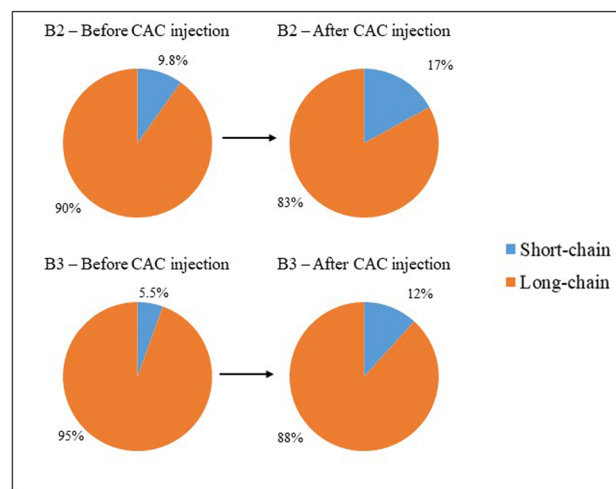


FIGURE 6 Change in groundwater concentrations for short- and long-chain PFAS after injection of CAC at the protection zone (well B2) and downstream (well B3). CAC, colloidal activated carbon; PFAS, per- and polyfluoroalkyl substances.

(Supporting Information: Figures S13 and S14). The plume from the east could also migrate under the stream, ending up on its west side. The geology of the site showed a zone of higher permeability till close to the bedrock (Supporting Information: Figure S3), which could serve as a communication channel for groundwater flow between the east and the west side of the stream (Figure 1).

Reductions in PFAS concentrations after the application of CAC were noticed mainly for long-chain PFAS, both in the protection zone (well B2) and downstream of it (well B3) (Figure 6). Taking the whole postinjection period into account (~21 months), including the rebound of concentrations, and comparing it with the average groundwater concentrations preinjection, the total reduction of Σ_{11} PFAS in groundwater was 52% (for details, see Supporting Information: Table S8). The highest decrease was noticed for PFOA (69%), followed by PFOS (58%) and PFBS (51%). The reduction of concentrations for individual PFCA and PFSA was visualized with radial diagrams (Carey et al., 2019) (Figure 7). It was evident that the PFAS most affected were PFSA and long-chain PFAS (PFOA and PFOS). These compounds are characterized by higher hydrophobicity, which can explain the higher sorption affinity to CAC resulting in higher removal from groundwater (Higgins & Luthy, 2006).

Temporal trends were noticed in the treatment's effectiveness. In the first 4 months after installation of the CAC PRB, there was an average reduction of 76% for Σ_{11} PFAS at the protection well (Period 1, Figure 8). The decrease was noticed mainly for long-chain PFAS and PFSA, while most short-chain PFAS, such as C₃–C₆ PFCA and PFBS, had a lower reduction. Specifically, in this first period, the highest reduction measured was for PFOS (83%), followed by PFOA (82%) and PFHxS (70%) and the lowest was for PFBA (50%). Despite a promising initial reduction, a high spike was detected approximately 5 months after the CAC injection (Period 2, Figure 8), with groundwater concentrations exceeding those on average before treatment for all

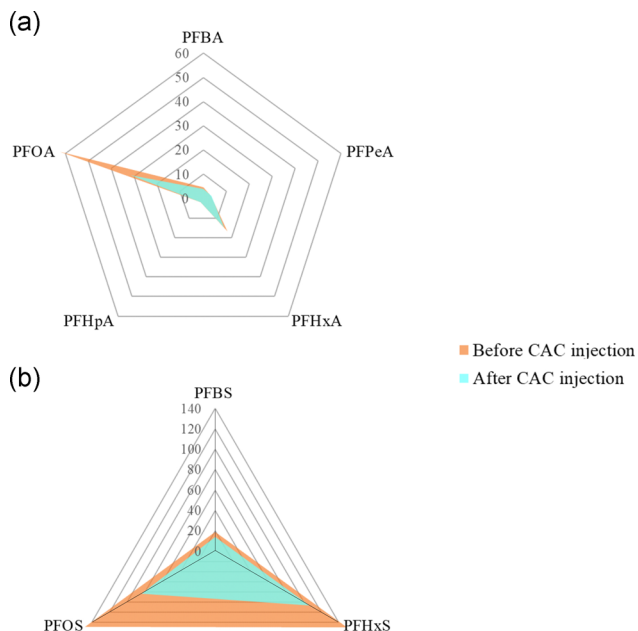


FIGURE 7 Radial diagrams comparing average groundwater concentrations (ng L^{-1}) at the protection zone (well B2) before and after CAC injection for (a) PFCA, and (b) PFSA. CAC, colloidal activated carbon; PFBA, perfluorobutanoic acid; PFBS, perfluorobutane sulfonic acid; PFCA, perfluorocarboxylic acids; PFHpA, perfluoroheptanoic acid; PFHxA, perfluorohexanoic acid; PFHxS, perfluorohexanesulfonic acid; PFOA, perfluorooctanoic acid; PFOS, perfluorooctane sulfonic acid; PFPeA, perfluoropentanoic acid; PFSA, perfluorosulfonates.

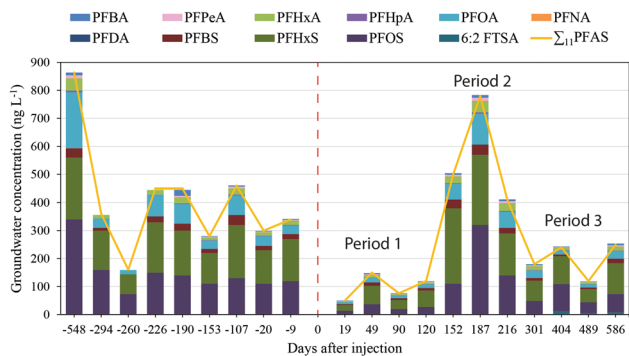


FIGURE 8 Concentrations of PFAS in groundwater at the protection well (B2). The red dashed line indicates the time when the CAC injection was completed. The three periods of postinjection are shown (Period 1: 19–120 days, Period 2: 152–216 days, Period 3: 301–586 days). CAC, colloidal activated carbon; PFAS, per- and polyfluoroalkyl substances; PFBA, perfluorobutanoic acid; PFBS, perfluorobutane sulfonic acid; PFHpA, perfluoroheptanoic acid; PFHxA, perfluorohexanoic acid; PFHxS, perfluorohexanesulfonic acid; PFOA, perfluorooctanoic acid; PFOS, perfluorooctane sulfonic acid; PFPeA, perfluoropentanoic acid.

PFAS. The same spike of concentrations was noticed at well B3, downstream of well B2, however, with a delay of 3.5 months (Supporting Information: Figure S15). The presence of other source zones contributing to the plume at the protection well was unlikely, considering the historical uses of the site (see Section 2.1). Groundwater monitoring continued after the rebound of concentrations, which eventually declined to levels lower than pre-injection and fluctuated less (Period 3, Figure 8).

Directly before injection, relatively high concentrations were noticed at the source zones (wells B1 and B8). This spike was likely due to seasonal variations affecting groundwater levels and concentrations (Figure 5). Therefore, the spike in concentrations at well B2 during Period 2 could be a delayed response to the maximum concentrations found at the source zones, in combination with the inability of the PRB to intercept the plume. According to the signatures, the highest increase in concentrations was detected for PFOS, indicating an intrusion of contaminated groundwater from the eastern source (well B8) (Figures 7 and 8). The injection of CAC also partially failed on the east side of the PRB, making it more susceptible to the plume coming from the east. As described previously, the water table in the barrier area was relatively flat, making it sensitive to changes in flow directions (Figure 3). Therefore, the prevailing theory to explain the spike of concentrations after injection is changing flow directions and plume intrusion from the primary source of contamination at well B8. At the well downstream of the PRB's protection zone (well B3), the concentrations only lowered for PFOS, showing that the barrier shielded partially from the PFOS source at B1 (Supporting Information: Figures S10 and S11). Conversely, PFOA concentrations increased to a lesser extent, indicating a better function of the PRB on the south side.

4 | CONCLUSIONS AND ENVIRONMENTAL IMPLICATIONS

Remediation of soil and groundwater with CAC has been proposed as one of the most promising materials for PFAS treatment. In this study, the field application of CAC was assessed at a PFAS-contaminated area of high geologic and hydrologic complexity, and plume intrusion from two separate source zones. Installation of the CAC barrier proved challenging due to the low permeability of the soil in combination with apparent high permeability channels deeper in the aquifer or fractures within the bedrock. A relatively flat groundwater table at the protection zone further complicated remedial efforts, showing sensitivity to seasonal variations and drilling operations. Despite these difficulties, the application of the barrier resulted in an overall 52% reduction of Σ_{11} PFAS in groundwater, while reduction rates reached 69% and 58% for PFOA and PFOS, respectively. The reduction was higher for long-chain PFAS and PFSA compared to other PFAS, in agreement with the results of other studies on CAC. The initial results showed a high drop in groundwater concentrations (76% for Σ_{11} PFAS);

however, a rebound of concentrations was observed 6 months after treatment. The main contributing factor to the rebound was considered to be the partial bypass of the PRB. Therefore, long-term monitoring is essential to understand the effectiveness of stabilization treatment with CAC. The longevity of a CAC barrier is directly proportional to the CAC fraction applied (Carey et al., 2022), therefore reapplication of CAC might be considered necessary in future scenarios.

The critical challenges presented in this study can serve as a guideline for pitfalls to be considered at similar sites. Specifically, hydrogeological aspects of the contaminated site need to be well understood before application of the treatment. For instance, the use of tracer tests before the treatment application could help to identify flow patterns. In addition, the geological conditions are key, since clay-rich aquifers can be sensitive to injection applications, even when it is performed at low pressures, due to the potential opening of new flow channels that can result in CAC losses. Redistribution of CAC and its elution from the aquifer can result in the escape of the plume to downstream locations. Based on the results of this case study, careful control of the CAC application is suggested, for example, by promoting aggregation using CaCl_2 and confirming the distribution of CAC through carbon analysis in the soil and groundwater. Another vital aspect to consider is potential changes in flow directions, either due to seasonal variations or the opening of new flow channels, which can lead to bypassing the PRB, especially at heterogeneous sites, such as the one presented herein. It is therefore key to have a complete understanding of a site's geological and hydrological parameters before application of CAC for PFAS soil and groundwater treatment.

ACKNOWLEDGMENTS

This work was financially supported by TUFFO—a research and innovation program on contaminated sites managed by the Swedish Geotechnical Institute (SGI)—through the StopPFAS project (1.1-1708-0501).

ORCID

Georgios Niarchos  <http://orcid.org/0000-0001-8318-1553>

REFERENCES

- ATDSR. (2018). Toxicological profile for perfluoroalkyls, draft for public comment. www.regulations.gov
- Brennan, N. M., Evans, A. T., Fritz, M. K., Peak, S. A., & von Holst, H. E. (2021). Trends in the regulation of per- and polyfluoroalkyl substances (PFAS): A scoping review. *International Journal of Environmental Research and Public Health*, 18(20), 10900. <https://doi.org/10.3390/IJERPH182010900/S1>
- Brusseau, M. L., Anderson, R. H., & Guo, B. (2020). PFAS concentrations in soils: Background levels versus contaminated sites. *Science of the Total Environment*, 740, 140017. <https://doi.org/10.1016/j.scitotenv.2020.140017>
- Carey, G. R., Hakimabadi, S. G., Singh, M., McGregor, R., Woodfield, C., Van Geel, P. J., & Pham, A. L. T. (2022). Longevity of colloidal activated carbon for in situ PFAS remediation at AFFF-contaminated airport sites. *Remediation Journal*, 33, 3–23. <https://doi.org/10.1002/REM.21741>
- Carey, G. R., McGregor, R., Pham, A. L. T., Sleep, B., & Hakimabadi, S. G. (2019). Evaluating the longevity of a PFAS in situ colloidal activated carbon remedy. *Remediation Journal*, 29(2), 17–31. <https://doi.org/10.1002/rem.21593>
- Crownover, E., Oberle, D., Kluger, M., & Heron, G. (2019). Perfluoroalkyl and polyfluoroalkyl substances thermal desorption evaluation. *Remediation Journal*, 29(4), 77–81. <https://doi.org/10.1002/REM.21623>
- Darlington, R., Barth, E., & McKernan, J. (2018). The challenges of PFAS remediation. *The Military Engineer*, 110(712), 58–60.
- Dauchy, X., Boiteux, V., Bach, C., Rosin, C., & Munoz, J.-F. (2017). Per- and polyfluoroalkyl substances in firefighting foam concentrates and water samples collected near sites impacted by the use of these foams. *Chemosphere*, 183, 53–61. <https://doi.org/10.1016/j.chemosphere.2017.05.056>
- Du, Z., Deng, S., Bei, Y., Huang, Q., Wang, B., Huang, J., & Yu, G. (2014). Adsorption behavior and mechanism of perfluorinated compounds on various adsorbents—A review. *Journal of Hazardous Materials*, 274, 443–454. <https://doi.org/10.1016/j.jhazmat.2014.04.038>
- Duffield, G. (2019). Hydraulic Properties: Aquifer Testing 101. http://www.aqtesolv.com/aquifer-tests/aquifer_properties.htm
- EWG & SSEHRI. (2019). Interactive map: PFAS contamination crisis: New data show 712 sites in 49 states. https://www.ewg.org/interactive-maps/2019_pfas_contamination/map/
- Guelfo, J. L., & Higgins, C. P. (2013). Subsurface transport potential of perfluoroalkyl acids at aqueous film-forming foam (AFFF)-impacted sites. *Environmental Science & Technology*, 47(9), 4164–4171. <https://doi.org/10.1021/es3048043>
- Hättestrand, C. (1997). Ribbed moraines in Sweden—Distribution pattern and palaeoglaciological implications. *Sedimentary Geology*, 111(1–4), 41–56. [https://doi.org/10.1016/S0037-0738\(97\)00005-5](https://doi.org/10.1016/S0037-0738(97)00005-5)
- Higgins, C. P., & Luthy, R. G. (2006). Sorption of perfluorinated surfactants on sediments. *Environmental Science & Technology*, 40, 7251–7256. <https://doi.org/10.1021/ES061000N>
- Høisæter, Å., Arp, H. P. H., Slinde, G., Knutsen, H., Hale, S. E., Breedveld, G. D., & Hansen, M. C. (2021). Excavated vs novel in situ soil washing as a remediation strategy for sandy soils impacted with per- and polyfluoroalkyl substances from aqueous film forming foams. *Science of the Total Environment*, 794, 148763. <https://doi.org/10.1016/J.SCITOTENV.2021.148763>
- Huang, D., Xiao, R., Du, L., Zhang, G., Yin, L., Deng, R., & Wang, G. (2021). Phytoremediation of poly- and perfluoroalkyl substances: A review on aquatic plants, influencing factors, and phytotoxicity. *Journal of Hazardous Materials*, 418, 126314. <https://doi.org/10.1016/J.JHAZMAT.2021.126314>
- Li, F., Fang, X., Zhou, Z., Liao, X., Zou, J., Yuan, B., & Sun, W. (2019). Adsorption of perfluorinated acids onto soils: Kinetics, isotherms, and influences of soil properties. *Science of the Total Environment*, 649, 504–514. <https://doi.org/10.1016/j.scitotenv.2018.08.209>
- Mackenzie, K., Schierz, A., Georgi, A., & Kopinke, F. D. (2008). Colloidal activated carbon and CARBO-IRON—Novel materials for in-situ groundwater treatment. *Global Nest Journal*, 10(1), 54–61. <https://doi.org/10.30955/GNJ.000506>
- Mahinroosta, R., & Senevirathna, L. (2020). A review of the emerging treatment technologies for PFAS contaminated soils. *Journal of Environmental Management*, 255, 109896. <https://doi.org/10.1016/j.jenvman.2019.109896>
- McGregor, R. (2020). Six pilot-scale studies evaluating the in situ treatment of PFAS in groundwater. *Remediation Journal*, 30(3), 39–50. <https://doi.org/10.1002/rem.21653>
- McGregor, R., & Benevenuto, L. (2021). The effect of heterogeneity on the distribution and treatment of PFAS in a complex geologic environment. *Frontiers in Environmental Chemistry*, 2, 729779. <https://doi.org/10.3389/FENVC.2021.729779>

- Niarchos, G., Lutz, A., Kleja, D. B., & Fagerlund, F. (2022). Per- and polyfluoroalkyl substance (PFAS) retention by colloidal activated carbon (CAC) using dynamic column experiments. *Environmental Pollution*, 308, 119667. <https://doi.org/10.1016/j.envpol.2022.119667>
- Niarchos, G., Söregård, M., Fagerlund, F., & Ahrens, L. (2022). Electrokinetic remediation for removal of per- and polyfluoroalkyl substances (PFASs) from contaminated soil. *Chemosphere*, 291, 133041. <https://doi.org/10.1016/J.CHEMOSPHERE.2021.133041>
- OECD. (2018). Toward a new comprehensive global database of per- and polyfluoroalkyl substances (PFASs): Summary report on updating the OECD 2007 list of per- and polyfluoroalkyl substances (PFASs) Series on Risk Management No. 39 JT03431231. [http://www.oecd.org/officialdocuments/publicdisplaydocumentpdf/?cote=ENV-JM-MONO\(2018\)7&doclanguage=en](http://www.oecd.org/officialdocuments/publicdisplaydocumentpdf/?cote=ENV-JM-MONO(2018)7&doclanguage=en)
- Petterson, M., Ländell, M., Ohlsson, Y., Kleja, D. B., & Tiberg, C. (2015). Preliminära riktvärden för högfluorerade ämnen (PFAS) i mark och grundvatten. www.swedgeo.se
- Ross, I., McDonough, J., Miles, J., Storch, P., Thelakkat Kochunaryanan, P., Kalve, E., Hurst, J., Dasgupta, S. S., & Burdick, J. (2018). A review of emerging technologies for remediation of PFASs. *Remediation Journal*, 28(2), 101–126. <https://doi.org/10.1002/rem.21553>
- Sorengard, M., Kleja, D. B., & Ahrens, L. (2019). Stabilization of per- and polyfluoroalkyl substances (PFASs) with colloidal activated carbon (PlumeStop®) as a function of soil clay and organic matter content. *Journal of Environmental Management*, 249, 109345. <https://doi.org/10.1016/j.jenvman.2019.109345>
- Söregård, M., Lindh, A. S., & Ahrens, L. (2020). Thermal desorption as a high removal remediation technique for soils contaminated with per- and polyfluoroalkyl substances (PFASs). *PLoS One*, 15(6), e0234476. <https://doi.org/10.1371/journal.pone.0234476>
- Söregård, M., Kikuchi, J., Wiberg, K., & Ahrens, L. (2022). Spatial distribution and load of per- and polyfluoroalkyl substances (PFAS) in background soils in Sweden. *Chemosphere*, 295, 133944. <https://doi.org/10.1016/J.CHEMOSPHERE.2022.133944>
- Söregård, M., Niarchos, G., Jensen, P. E., & Ahrens, L. (2019). Electrodialytic per- and polyfluoroalkyl substances (PFASs) removal mechanism for contaminated soil. *Chemosphere*, 232, 224–231. <https://doi.org/10.1016/j.chemosphere.2019.05.088>
- Swedish Environmental Protection Agency. (2016). Högfluorerade ämnen (PFAS) och bekämpningsmedel. Naturvårdsverket. <https://www.naturvardsverket.se/978-91-620-6709-0>
- The European Parliament and the Council of the European Union. (2020). Directive 2013/11/EU of the European Parliament and of the Council of 12 August 2013 amending Directives 2000/60/EC and 2008/105/EC as regards priority substances in the field of water policy. In *Fundamental Texts On European Private Law*, July 2013. <https://doi.org/10.5040/9781782258674.0032>
- Wang, Z., Cousins, I. T., Scheringer, M., Buck, R. C., & Hungerbühler, K. (2014). Global emission inventories for C₄–C₁₄ perfluoroalkyl carboxylic acid (PFCA) homologues from 1951 to 2030, Part I: Production and emissions from quantifiable sources. *Environment International*, 70, 62–75. <https://doi.org/10.1016/J.ENVINT.2014.04.013>

AUTHOR BIOGRAPHIES

Georgios Niarchos, PhD, is a postdoctoral researcher at the department of Aquatic Sciences and Assessment at the Swedish University of Agricultural Sciences, Uppsala, Sweden. His research focuses on PFAS contamination, emphasizing

remediation techniques for soil and groundwater, as well as fate and transport of PFAS in environmental media. He holds a PhD in Hydrology from the University of Uppsala, Sweden, an MSc in Environmental Engineering and Sustainable Infrastructure from the Royal Institute of Technology KTH, Sweden, and an MEng in Environmental Engineering from the Technical University of Crete, Greece.

Lutz Ahrens, PhD, is an Associate Professor at the Department of Aquatic Sciences and Assessment at SLU, Sweden. His research interests include sources, fate, and transport of emerging organic pollutants in the environment, the development of suspect and nontarget screening methods, and the development of advanced treatment techniques for soil and water.

Dan Berggren Kleja, PhD, is a Professor of Soil Chemistry at the Swedish University of Agricultural Sciences (SLU) and a researcher at the Swedish Geotechnical Institute. His present research includes contaminant transport and fate in soils and groundwater, as well as the development of novel soil and groundwater remediation methods for contaminants, including PFAS.

Gareth Leonard, MSc, is the Managing Director of REGENESIS in Europe. He received a BSc in Geology from Leeds University and an MSc in Environmental Chemistry from Northumbria University. Gareth has over 20 years contaminated land experience, remediating sites in Europe, the Middle East, and Africa.

Jim Forde, MSc, is the Technical Manager for UK and Scandinavia at REGENESIS in Europe, where he is responsible for groundwater remediation designs for a range of contaminants, including PFAS. He received a BSc in Environmental Science from the University of Nottingham and an MSc in Hydrogeology from the University of Birmingham. Jim has over 10 years contaminated land experience, remediating sites in Europe and North America.

Jonny Bergman, BSc, is an expert on in-situ remediation technologies with more than 25 years of experience. His expertise has included planning and design of prerediation site investigations, pilot tests, and full-scale application of most known in-situ remediation technologies. He has also been involved in the development of in-situ remediation technologies targeting all predominant contaminants and geological conditions in the Nordic region.

Erik Ribeli, MSc, is working as an environmental consultant and PFAS Specialist. He received his master's degree in environmental engineering from Uppsala University in 2014 and has been working with different remediation projects throughout Scandinavia since then.

Matilda Schütz, MSc, is an environmental consultant at NIRAS Sweden AB. Her focus is in PFAS contaminated sites with focus

on soil and groundwater. She received her BSc in Geosciences from Uppsala University and her MSc in Environmental geology from Gothenburg University.

Fritjof Fagerlund, PhD, is a Professor in Geohydrology at Uppsala University, Sweden. His research interests include subsurface flow and transport processes, in particular with regard to contaminants in soil and groundwater and the development of novel mitigation methods. He is currently working on projects on PFAS remediation. He has an MS in Environmental Engineering and a PhD in Hydrology from Uppsala University.

SUPPORTING INFORMATION

Additional supporting information can be found online in the Supporting Information section at the end of this article.

How to cite this article: Niarchos, G., Ahrens, L., Kleja, D. B., Leonard, G., Forde, J., Bergman, J., Ribeli, E., Schütz, M., & Fagerlund, F. (2023). In-situ application of colloidal activated carbon for PFAS-contaminated soil and groundwater: A Swedish case study. *Remediation*, 33, 101–110. <https://doi.org/10.1002/rem.21746>